

We are IntechOpen, the world's leading publisher of Open Access books Built by scientists, for scientists

5,400

Open access books available

132,000

International authors and editors

160M

Downloads

Our authors are among the

154

Countries delivered to

TOP 1%

most cited scientists

12.2%

Contributors from top 500 universities



WEB OF SCIENCE™

Selection of our books indexed in the Book Citation Index
in Web of Science™ Core Collection (BKCI)

Interested in publishing with us?
Contact book.department@intechopen.com

Numbers displayed above are based on latest data collected.
For more information visit www.intechopen.com



Review – Metallic Bipolar Plates and Their Usage in Energy Conversion Systems

Justin Richards and Kerstin Schmidt
*Fraunhofer Institute for Chemical Technology,
Project Group Sustainable Mobility, Wolfsburg,
Germany*

1. Introduction

“Fuel cells, like batteries, are electrochemical galvanic cells that convert chemical energy directly into electrical energy and are not subject to the Carnot cycle limitations of heat engines.” [48] Unlike batteries the active material for fuel cells is externally stored which allows capacity and power to be scaled independently.

1.1 History

The first primary battery was invented by Alessandro Volta in 1800, the “Volta Pile” [70]. The first secondary battery which gave the basis for the lead-acid batteries found in most of the automotive applications was developed in 1859 by Raymond Gaston Planté [55].

The idea of a fuel cell was first discovered in 1839 by Christian Friedrich Schönbein [64] and William Grove [27]. Independently from each other they provided the foundation for the development of many different kinds of fuel cells. Today’s fuel cells are mostly classified by the type of electrolyte used in the cells. The most common types are polymer electrolyte fuel cells PEFC (developed by William Grubb in 1959), the alkaline fuel cell AFC (developed for the Apollo space Program in the 1960’s), the phosphoric acid fuel cell PAFC (from 1965), the molten carbonate fuel cell MCFC and the solid oxide fuel cells SOFC. The beginnings of SOFC and MCFC can be dated back to the mid 1960’s [23].

1.2 Importance of fuel cells

Global warming and the political situation pushed the focus further to the renewable energy sources such as wind and solar energy. Their discontinuous availability conflicts with the required energy need. To compensate the increasingly temporary imbalance between generation and demand of energy, innovation solutions must be found. A better adjustment of the reserves to meet the changing demands can be achieved by using decentralized storage devices. The electrolysis of water and the storing of hydrogen in tanks is a promising solution. At times where the demand for energy is high, the hydrogen can be used to supply fuel cells where it will be recombined with oxygen from the air generating electricity. Besides the stationary applications in combination with electrolyzer, fuel cells

operating on hydrogen are a promising option for the electrical energy supply for passenger cars with electrical drive trains and medium operating ranges. Due to their high power density and fast start-up time, proton exchange membrane fuel cells show highest potential for automotive applications [23].

1.3 Assembly

Fuel cells are generally assembled according to the stack method (shown in Fig.1).

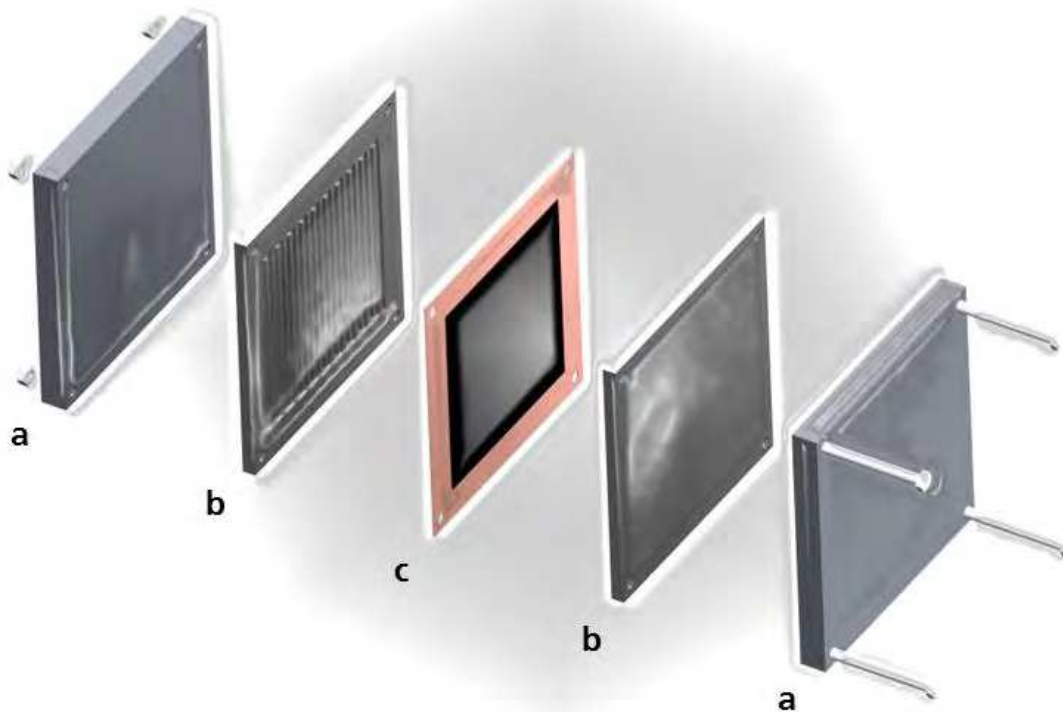


Fig. 1. Schematic design of a one cell stack

The endplates apply the necessary pressure on the stack (a). The bipolar plates (b) define about 60 % of the weight and about 30 % of the cost of one cell. They also provide conduits for the gas and fluid flows of reactants and products of a cell. They remove heat from the active areas and carry it current from cell to cell. The plates also constitute the backbone thus the mechanical stability of a stack. The two half cells are separated by an ionic conductor (c). Depending on the application it mostly is coated with a carbon supported catalyst.

To gain high voltages from a fuel cell the current collector plates of a cell, sometimes known as interconnectors (in SOFCs), are designed to be used as bipolar plates. One side supports the anode and the other side the cathode for the next cell. They are electrically connected in series (Fig. 2). The power (P) output of a fuel cell stack can be calculated by multiplication of the sum of the voltage differences (ΔU) and the current (I)

$$P[W]=I[A] \cdot \sum \Delta U[V] \quad (1)$$

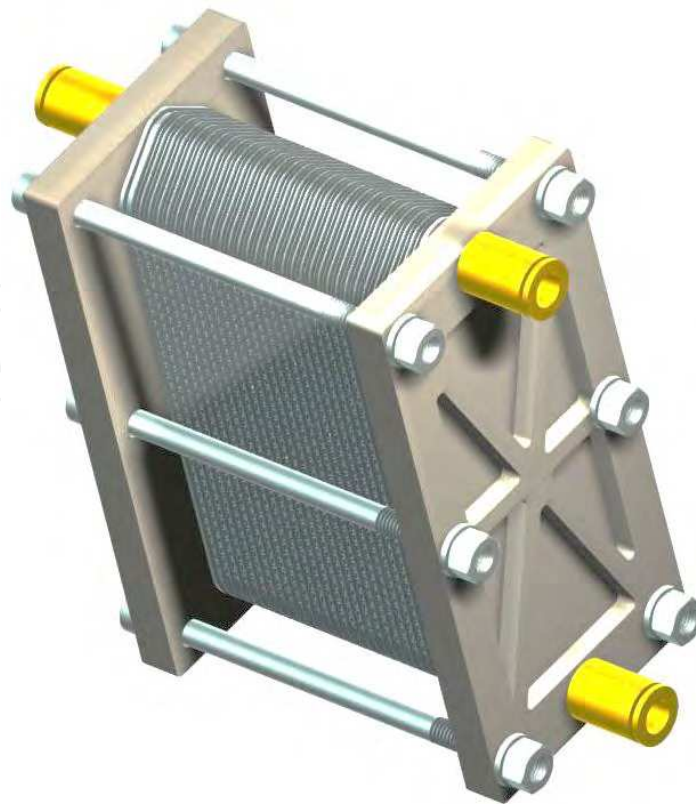


Fig. 2. Schematic design of an air-breathing PEMFC stack

1.4 Graphite – The state of the art material for bipolar plates

Currently graphite and graphite composites are considered the standard material for bipolar plates in e.g. PEMFC. This material provides a good electrical conductivity, a low contact resistance and an outstanding corrosion resistance [2]. However the mechanical properties of graphite limit the design and the dimensions of a stack. With a conductive electrolyte present, electro migration of ions into the graphite structure can take place which results in an expansion of the plate thus lowering the mechanical strength of the graphite. Other disadvantages of graphite are its permeability (e.g. for hydrogen) and its poor cost effectiveness for high volume manufacturing processes compared to metals such as stainless steels.

Recent fuel cell developments comply with the volumetric and gravimetric power density criteria ($>1 \text{ kW/l}$ and $>1 \text{ kW/kg}$) [2]. The two major challenges hindering the technology to gain a firm footing in the energy market, the costs of a fuel cell and its durability.

1.5 Targets of the Department of Energy (DOE) for metallic bipolar plates

“The Department of Energy sets goals for all new technologies. Through R&D and technology validation programs, DOE gathers and reports progress towards the goals”. [9]

Metals both treated and untreated are promising candidates for the usage as bipolar plates. However their low corrosion resistance and their high contact resistance resulting from the oxide layer formed on its surface hinder the general use in PEMFCs [37].

Parameter	Unit	DOE Targets		
		2005 Status	2010	2015
Plate Cost	\$/kW ⁻¹	10	5	3
Plate Weight	Kg/kW ⁻¹	0,36	<0,4	<0,4
H ₂ Permeation rate	cm ³ s ⁻¹ cm ⁻²	<2*10 ⁻⁶	<2*10 ⁻⁶	<2*10 ⁻⁶
Corrosion ¹	μA*cm ⁻²	<1	<1	<1
Resistance ²	Ohm*cm ²	<0,01	<0,02	<0,02
Resistivity [72]	Ohm*cm	-	<0,01	<0,01
Flexural Strength	MPa	>34	>25	>25
Flexibility	%	1.5 – 3.5	3 – 5	3 – 5
Durability with cycling [74]	h	-	5000 ³	-

¹Electrolyte consist of pH 3 H₂SO₄ + 0.1 ppm hydrofluorhydric acid (HF) solution under 0.8 V (NHE) at 80 °C (Pontentiostatic Corrosion Current)

²Resistance including the contact resistance at 140 N/cm²[74]; ³<10% drop in power

Table 1. DOE Metal Plate Status and DOE's Targets

The corrosion of the metallic plates can result in a degradation of the membrane due to the affinity of the proton conducting groups in the membrane to adsorb the leached ions from the metal surface [69]. Furthermore the passive layers formed on the metal bipolar plates guard them from most corrosion attacks but increase the electrical resistivity. Consequently the fuel cell's efficiency declines as the oxide layers grow [3]. Therefore the department of energy states target values for various metallic bipolar plate parameters which are listed in Table 1 [75].

2. Material requirements

The material challenges are different for each energy conversion system. Operating temperatures, leached ions or different fuels have a great effect on the used components. The following chapter will give a brief overview on some of the types of energy conversion systems and on the theoretically used environment displaying them.

Low temperature proton exchange membrane fuel cell (LT-PEMFC)

Operating temperature	60 °C - 80 °C
Reacting agents	Air, oxygen , hydrogen
Operating pressure	1 bar to 3 bar absolute

Electrolyte solutions used for corrosion tests displaying PEMFC environments contain sulfate and mostly fluoride ions. The ions are the result of the degradation of the membrane and can be found in the effluent water [86]. The electrolyte is also purged with air displaying the cathode side or purged with H₂ displaying the anode side. The concentrations of sulfate-ions in the solutions vary from 0,001 mol*l⁻¹ up to 1 mol*l⁻¹. Most electrolytes also exhibit fluoride ions at concentration up to 2 ppm. The corrosion tests are realized at different temperatures from ambient temperature up to 80 °C [3].

High temperature proton exchange membrane fuel cell (HT-PEMFC)

Operating temperature	120 °C - 180 °C
Reacting agents	Air, oxygen , hydrogen
Operating pressure	1 bar to 3 bar absolute

To overcome the challenges of the water and thermal management for LT-PEMFC several attempts have been made to develop so called high-temperature PEMFCs, which would operate in the temperature range 120 °C to 160 °C [23], [65]. The elevated temperatures cause great challenges for the applied materials. Additionally the proton conductivity of the membrane used in HT-PEMFCs has to be realized differently unlike using H₂O in LT-PEMFC membranes. Different approaches are known in the literature [89]:

- Modified PFSA membranes
- Sulfonated polyaromatic polymers and composite membranes (PEEK, sPEEK)
- Acid-based polymer membranes (phosphoric acid-doped PBI).

For each approach the simulated corrosion environment changes. For example bipolar plate material tests for doped PBI are pickled in 85 % phosphoric acid at 160 °C for 24 hours. [89]

Solid oxide fuel cell (SOFC)

Operating temperature	600 °C - 1000 °C
Reacting agents	Air, oxygen, hydrogen
Operating pressure	~10 bar

The basis for the SOFC was the discovery of Nernst in 1890. He realized that some perovskites were able to conduct ions in certain temperature ranges [23].

The interconnectors used in SOFCs can be divided into two categories, ceramics and metal alloys. The Ceramics are used at temperatures around 1000 °C whereas the metals can be found in applications with temperatures around 650 °C to 800 °C. The metals have to withstand the thermal cycling while still providing adequate contact resistances [19]. To investigate the durability of the metals Ziomek-Moroz [91] treated metal tubes in 99 % N₂ and 1 % H₂ for one year at temperatures of 600 °C, 700 °C and 800 °C analyzing the effects on the metal specimen afterwards.

Direct methanol fuel cell (DMFC)

Operating temperature	40 °C - 80 °C
Reacting agents	Air, methanol
Operating pressure	Ambient

The DMFCs are mostly used for portable applications [23]. Corrosion properties of materials for bipolar plates can be analyzed in a theoretical environment consisting of a 0.5 M H₂SO₄ solution with 10 % methanol [47].

3. Precious metals

Precious metals such as platinum and gold provide excellent corrosion resistance as well as good electrical conductivity [37], [84]. Nevertheless the costs for gold tripled in the last decade and is now as high as ~1065 €/ounce [80]. Platinum had an intermediate peak in 2008 with around 2200 €/ounce. Today's price for one ounce is around 1800 € [79]. These high prices prohibit the utilization of these metals as bipolar plate material for commercial use. Table 2 compares the costs of gold and other usable materials.

Material	Material cost (US \$/g)	Density (g/cm ³)
Graphite	0.105	1.79
Aluminum	0.0088	2.7
Gold	9.97	19.32
Electroless nickel	0.034	8.19

Table 2. Bipolar plate material and high-volume material costs [37]

4. Stainless steel alloys

To further increase the power density of fuel cells and to decrease the costs of the stacks, the use of very thin steel bipolar plates which can be formed in a low cost hydroforming process would be beneficial.

4.1 Untreated

The major concerns for bulk metal alloys are the corrosion resistance against the harsh environment and the resulting increase in contact resistance once the passive layer forms on the surface.

Many different alloys have been tested for the use as bipolar plate materials in fuel cells. Herman et al. [31] reports that aluminum, titanium, stainless steels and nickel exposed to a PEMFC-like environment exhibit corrosion and dissolution. While a protective layer forms on the surface of the metal specimen to provide protection against the corrosion attacks, the contact resistance increases thus lowering the overall performance of the stack.

Davies et al. [14] indicates that compared to tested metal alloys the graphite material exhibits the lowest interfacial resistance. The resistance values (measured with a compaction force of 220 N/cm² similar to the force imposed in a fuel cell) of the metal alloys decrease in the order 321¹ > 304¹ > 347¹ > 316¹ > Ti > 310¹ > 904¹ > Incoloy 800¹ > Inconel 601¹ > graphite. The influence on the surface resistivity depends on the compression force seen in Fig. 3. Kraysberg [39] suggests that texturing the bipolar plate surface would improve contact points thus reducing the resistivity.

4.2 Surface treatments

To improve corrosion resistance, steels can be provided with some kind of corrosion protection [13], [28], [56], [58], and [60]. Richards et al. [61] reported corrosion-test results of stainless steel specimen treated with a commercial coating solution (CCS) in combination with physicochemical surface treatments, electro-polishing and thermal annealing. Fig. 4 displays an improvement for the electro-polished and thermal annealed sample at high potentials. The other treated test specimen showed even higher corrosion currents than the bulk material.

¹Metall alloys are named with their symbol or material number by European standards DIN EN 10027 [90]

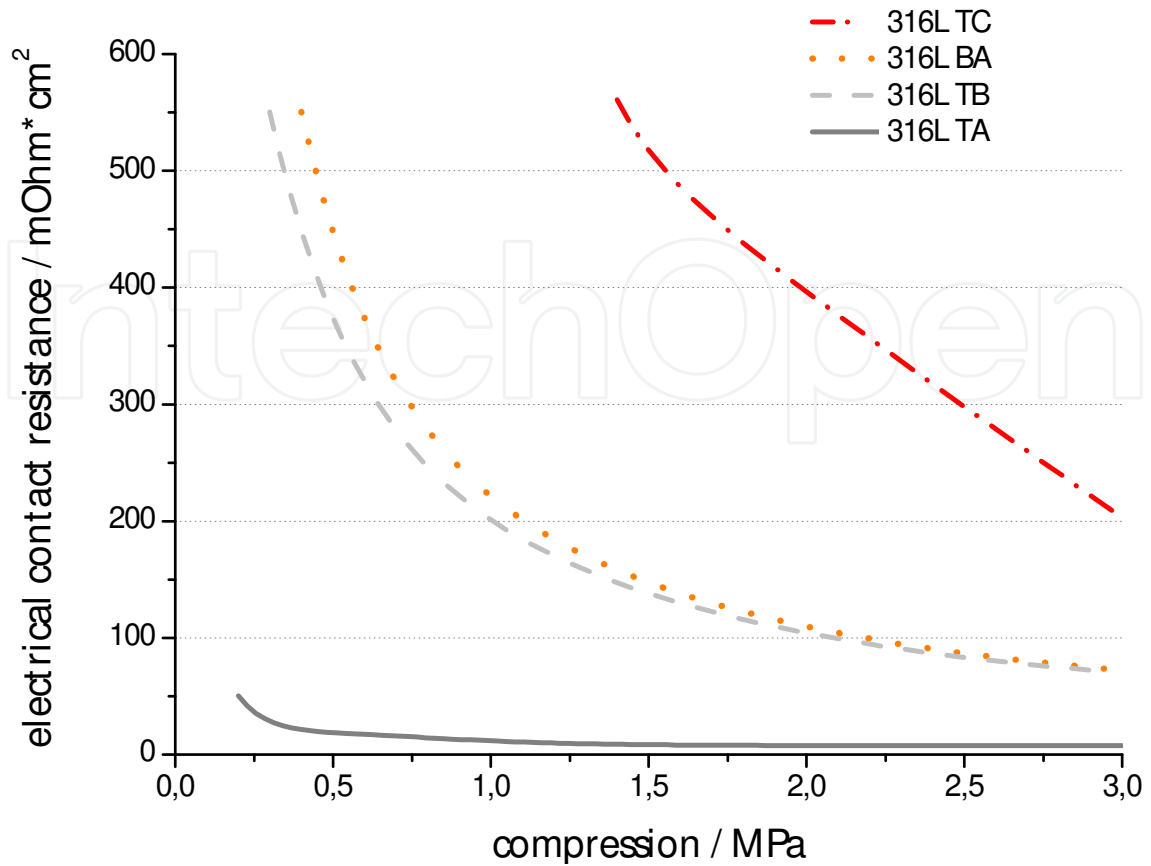


Fig. 3. Qualitative diagram of the electrical contact resistance of 316L samples for different pressure values [1]

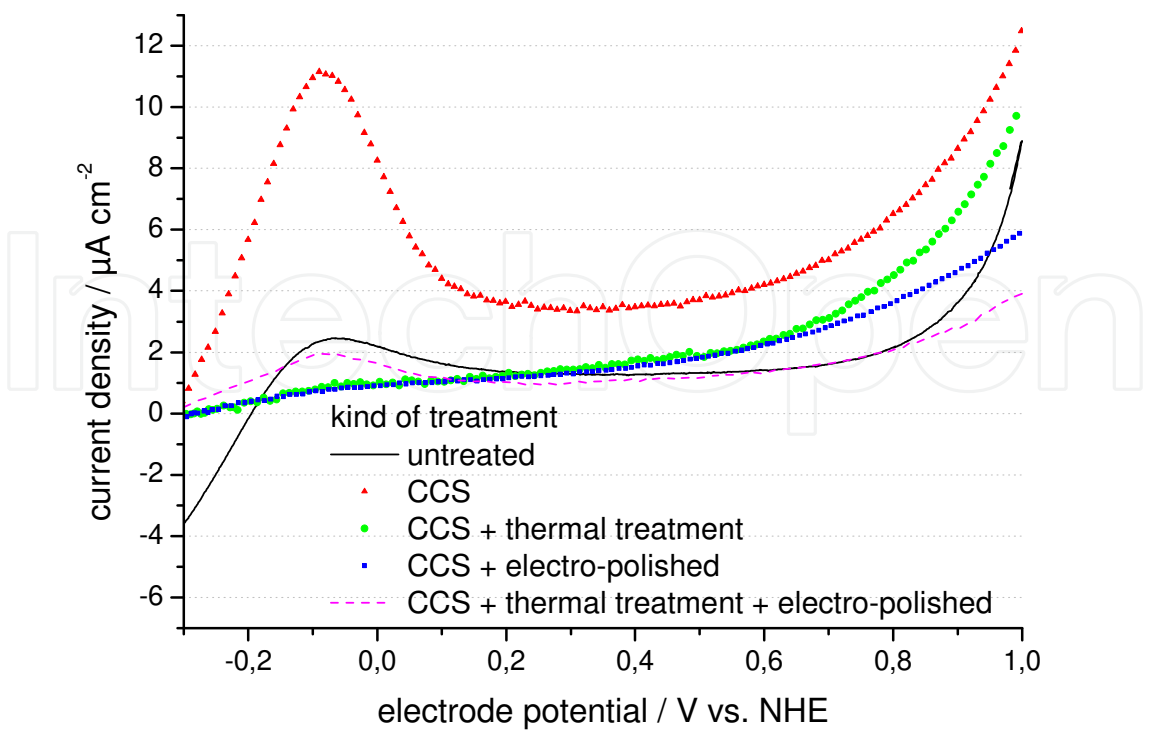


Fig. 4. LSV of alloy 2.4605 after different surface treatments at 50 °C [61]

The electro-polishing of stainless steels is an electrochemical surface treatment which is widely used for decorated utilization as well as for applications in medical and food science. The work done by Lee [44] provided results to the application of electro-polishing on stainless steels for bipolar plates. He used electrochemical surface treatments on 316L and reported that the content of chrome increased significantly in the passive layer on the specimen thus decrease the corrosion currents.

4.3 Amorphous metal alloys

Metal alloys or metallic glasses were first discovered in 1960 where Klement Willens and Duwes [67] reported the synthesis of amorphous metals by rapidly quenching (10^6 K) an Au-Si alloy from ~ 1300 °C to room temperature. To reduce the cooling rate and the material costs new alloys were developed. In 1995 the first iron based bulk metallic glasses was invented. One of the crucial aspects to design new amorphous alloys is that the difference in atomic size must be greater than 12 % [50].

Jayaraj [34], [33] compared the properties of the alloys $\text{Fe}_{48}\text{Cr}_{15}\text{Mo}_{14}\text{Y}_2\text{C}_{15}\text{B}_6$, $\text{Fe}_{44}\text{Cr}_{16}\text{Mo}_{16}\text{C}_{18}\text{B}_6$ and $\text{Fe}_{50}\text{Cr}_{18}\text{Mo}_8\text{Al}_2\text{Y}_2\text{C}_{14}\text{B}_6$ to a standard alloy 316L. Unfortunately he discovered that despite their unique properties, such as high strength, good hardness, good wear resistance, and high corrosion resistance, the amorphous alloy did not meet the DOE targets. In 2006 Jin, S. et al [35] detected a four times lower corrosion current of $\text{Zr}_{75}\text{Ti}_{25}$ ($0.021 \mu\text{A}/\text{cm}^2$) compared to 316L after a period of 5 hours at 80 °C in simulated anodic PEMFC environment. He also reported that 316L and $\text{Zr}_{75}\text{Ti}_{25}$ showed a considerable difference on forming an oxide film on their surface (Fig. 5).

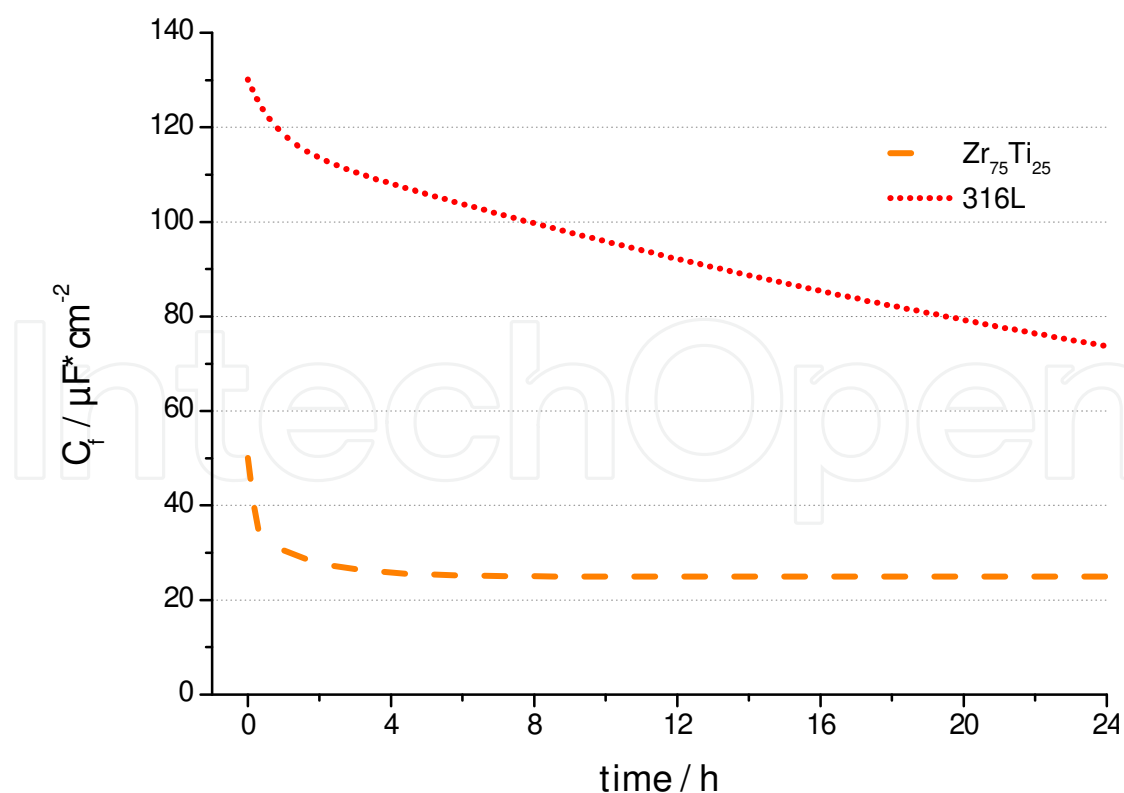


Fig. 5. Qualitative diagram of the oxide film capacity of 316L and $\text{Zr}_{75}\text{Ti}_{25}$ in the acid solution bubbled with H_2 at 25 °C [35]

5. Coated metals

Coatings for metallic bipolar plates should be conductive and adhere to the substrate material with little to no porosity [37].

5.1 Electroplating

The conductive substrate material is dipped into an electrolyte bath containing dissolved metal ions. By connecting the substrate as cathode the dissolved ions are deposited on the surface.

Walsh et al. [71] investigated the influence of the porosity of electrochemically deposited metal coatings on the corrosion properties of the specimen. Fig. 6 indicates a rapid decrease of the corrosion rate of nickel coatings on aluminum with increasing thickness of the layer. From a thickness of $\sim 2.5 \mu\text{m}$ a horizontal region indicates a pore free passive film [71].

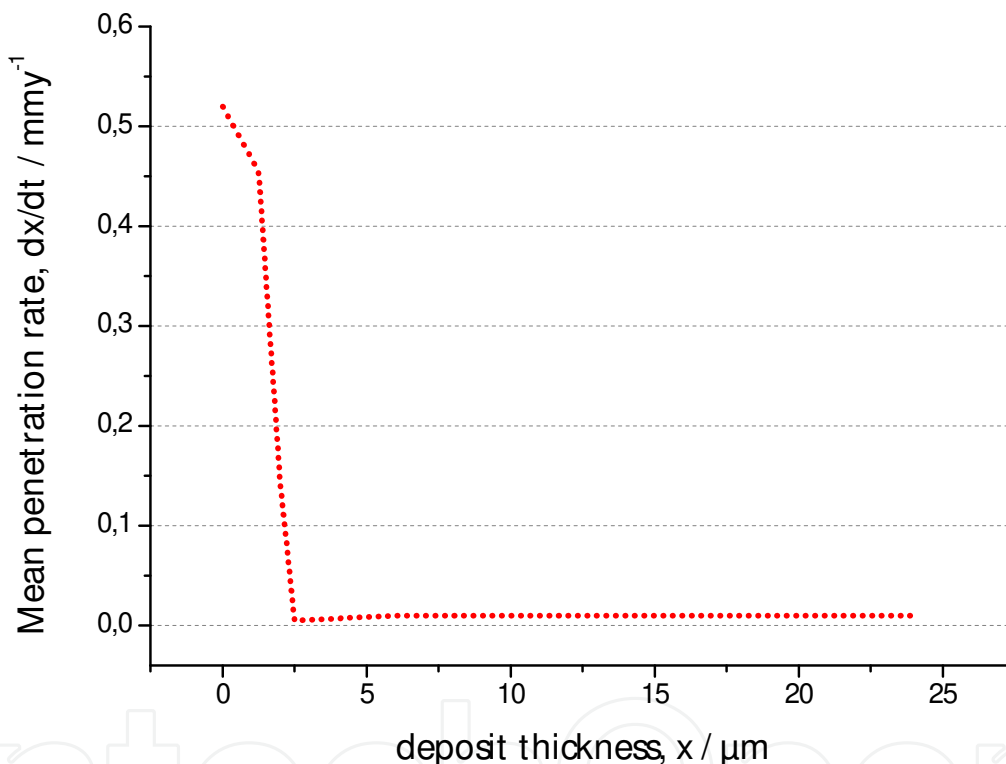


Fig. 6. Qualitative corrosion rate vs. electroless nickel coating thickness on aluminium in 0.85 mol/dm^3 (5%) NaCl at 295 K [71].

Hental et al. [29] coated an aluminum substrate material with gold. First tests showed an almost equal performance to graphite (1.2 A/cm^2 at 0.7 V). But very quickly the performance dropped to 60 mA/cm^2 at 0.5 V. Subsequent analysis revealed that parts of the gold layer had been lifted off the surface and became embedded in the membrane. Other tests by Yoon et al. [88] indicated very good performance of gold coated 316L. The DOE targets for corrosion currents in an anodic environment and for the contact resistance were met with 316L coated with 10 nm gold. But only the ZrNAu coating on 316L showed satisfying results in the cathode environment.

El-Enin et al. [18] investigated aluminum as substrate material with different electro-deposited coatings. His results show that the Ni-Co coating exhibits the best corrosion

properties due to its structure. Showing good performances in corrosion resistance as well the author recommends Ni-Mo-Fe-Cr coating with further annealing to be applied in a fuel cell instead of graphite.

5.2 Chemical vapor deposition

“Chemical vapor deposition may be defined as the deposition of a solid on a heated surface from a chemical reaction in the vapor phase.” [54]

Another approach for stabilizing metallic bipolar plates in energy conversion environments is to deposit good conducting and inert material compositions onto the metal surfaces. In 2009 Chung and colleagues [12] investigated coatings of carbon, formed from a C_2H_2/H_2 gas mixture at 690 °C to 930 °C on SUS304 metal substrates.

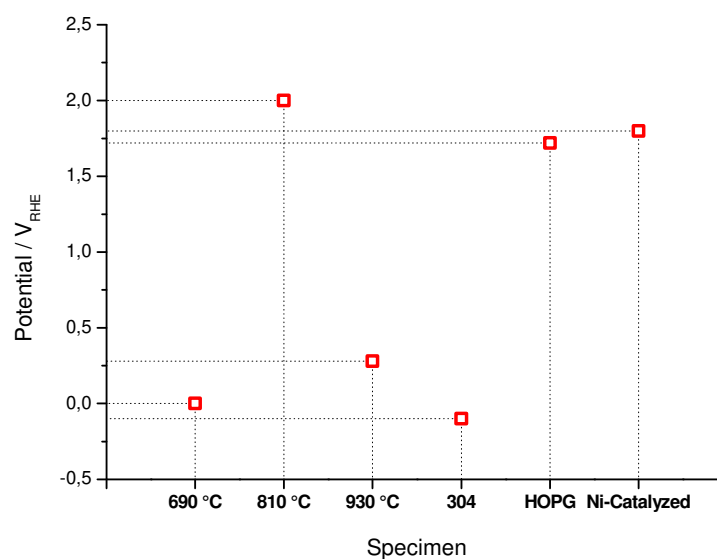


Fig. 7. Corrosion potential of specimen tested in 0.5 M H₂SO₄ solution at 25 °C [11]

All reported carbon films in this study showed an improved resistivity for the metal plates to a level comparable to the highly oriented pyrolytic graphite (HOPG). The results show a significant influence of the temperature range of the treatment on the corrosion potentials of the specimen. The specimen prepared at a temperature of 810 °C exhibits the highest corrosion potential followed by the Ni-catalyzed, the HOPG and the specimen prepared at 930 °C. The sample coated at 690 °C showed a little higher corrosion potential than the bulk specimen. The results for the corrosion potentials for the tested samples are displayed in Figure 7.

Good properties for the use in energy conversion systems can also be provided by chromizing metal surfaces. Lee et al. [42] investigated a chromizing process for 316L by CVD enhanced pack cementation. They used two different powder mixtures consisting of 50 % Cr, 43 % Al₂O₃ (A) and 7% NH₄C respectively 25 % Cr, 72 % Al₂O₃ and 3 % NH₄C (B). The corrosion resistance improved compared to the bulk material. The interfacial contact resistance was significantly influenced by the composition and procedure of the chromizing process. Specimen A exhibits the highest resistance in the test. It was up to three times higher (~50 Ohm*cm²) than the resistance of the bulk specimen and the specimen B resulting from the absence of the chrome carbide in the outer surface layer. Wen et al. [81] reported that modified SS420 chromized by a low temperature process possessed a reduction of four to

five orders of magnitude when compared with its bulk substrate ($100 \mu\text{A}/\text{cm}^2$ - $10 \mu\text{A}/\text{cm}^2$). The contact resistances value at $12\text{-}18 \text{ m}\Omega\cdot\text{cm}^2$ was below those of Lee [42] and colleagues released in 2009. Other experiments by Bai et al. [5] showed an influence on the pretreatment of AISI1020 as the substrate material which was also chromized by pack cementation. With electrical discharge machining (EDM) as pretreatment these specimen showed corrosion potentials little higher ($-0,45 \text{ V}$ and 0.37 V vs. SCE^2) than that of the bulk substrate ($\sim 4.5 \text{ V vs. SCE}$) but with little contact resistances ($11.8 \text{ m}\Omega\cdot\text{cm}^2$ and $17.7 \text{ m}\Omega\cdot\text{cm}^2$).

5.3 Physical vapor deposition

In the physical vapor deposition processes (PVD) or thin film processes a solid or liquid material is vaporized by e.g. electron beams and is deposited onto the surface of a substrate. Thin films of a few nanometers to a thousand nanometers can be achieved. Multilayers and free standing structures like ribs are also possible [49].

Stainless steel specimen used as substrates in PVD processes need to be pretreated by sputtering the surface with e.g. Ar-ions which remove the passive film on the material. Fu et al. [21] investigated three different carbon based films for the use as bipolar plate materials. The C-Film and the C-Cr-N-film exhibited relatively high contact resistances. The C-Cr deposited film provided a good corrosion resistance little higher than the DOE-targets and much lower contact resistance ($\sim 10 \text{ m}\Omega/\text{cm}^2$) than the other tested samples. Dur et al. [17] showed the effect of the manufacturing process on the corrosion resistance of modified stainless steel samples. The specimen were formed by stamping or hydroforming into bipolar plates and subsequently coated with TiN, CrN and ZrN. Among the coated samples the corrosion resistance was best for ZrN followed by CrN and TiN. Surprisingly TiN coated samples showed even lower resistances than their bulk samples. Regardless of the coating type the blank unformed samples provided the highest corrosion resistance. Wang, Y. [77] states that besides a corrosion resistant coating the substrate itself should have a high corrosion resistance. Those results were gained by tests with 316L and SS410 coated with TiN.

Investigations on a Ni-Cr enriched layer by Feng K. [19] with a thickness of 60 nm showed an improvement in corrosion resistance and a decrease in interfacial resistance. However the results are not at the desired level for PEMFC applications. A different solution was provided by Cha [11] who reported that a multiphase NbN/NbCrN film performed better than a single phased NbN film as a coating for metallic bipolar plates. The specimens were fabricated by sputtering Nb, Cr and using N_2 as reaction gas. Cha states that concerning the interfacial resistance the chromium amount in the layer does not make much of a difference but the influence in the gas ratio is noticeable. The corrosion resistance improved significantly compared to the bare material but pitting corrosion appears with certain coating process parameters. In the work done by Zhang et al. [90] it is shown that the corrosion resistance as well as the electrical conductivity and also the mechanical properties (hardness) are increased by arc ion plating. Zhang and colleagues coated 316L with a multilayer consisting of Cr/CrN/Cr.

²SCE – saturated calomel electrode

Lee et al. [43] coated aluminum (PVD coating of diamond-like film on 5052 Al) with the bulk 316L, bulk Al and graphite. The results were displayed in a tafel plot. The corrosion resistance of the coated samples is higher than its uncoated substrate but not as good as the 316L specimen. But the treated Al samples exhibits lower contact resistance than the 316L thus increasing the power of the cell.

5.4 Diffusion coating with Nitride

Different approaches by nitridation or nitrating steel samples can be found in the literature. Yang et al. [87] modified the surface of Fe-27Cr-6V and Fe-27Cr-2V alloy with high temperature nitridation. Their published results showed good corrosion and low interfacial resistances for the prepared samples. They also discovered that the addition of vanadium in the specimen influence the external nitride layer positively. A TEM cross section image of the nitride surface structure can be seen in Fig. 7. Improvements of contact resistances for a thermally nitride AISI446 stainless steel alloy at 1100 °C for 24 h was shown in the reported work of Wang H. et al. [73]. An increase in corrosion resistance was also observed for the cathodic environment. Unfortunately it exhibited poor corrosion resistance properties in the anodic conditions.

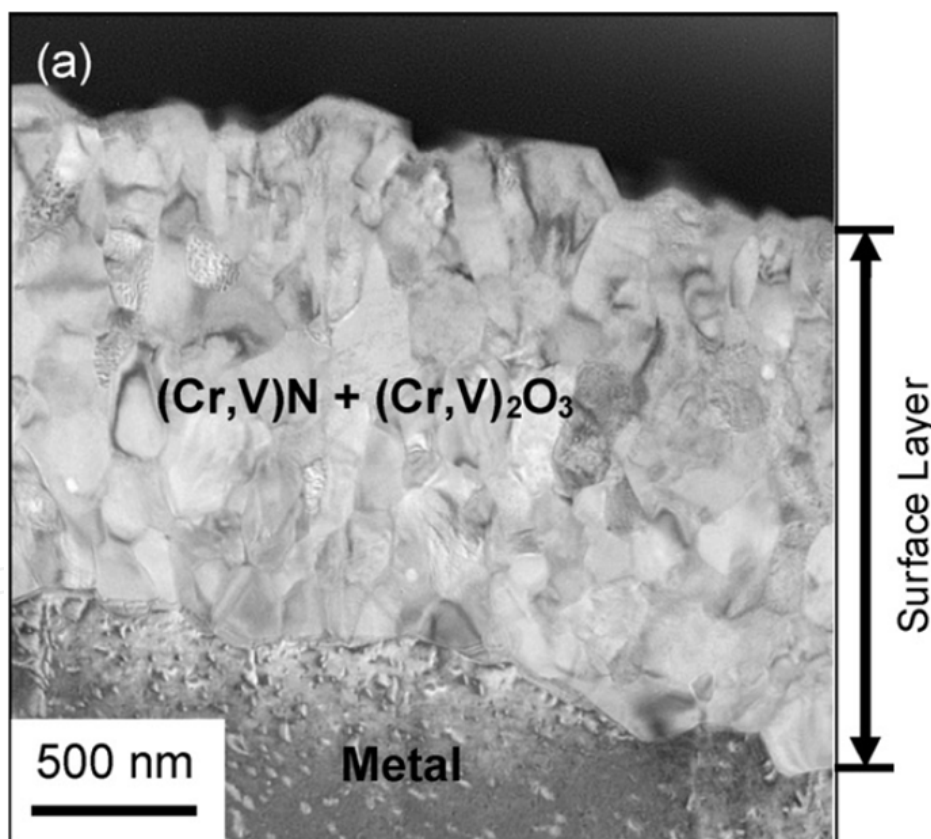


Fig. 8. Microstructures of nitrided Fe-27Cr-6V (850 °C, 24 h, N₂-4H₂) bright-field cross-section TEM [87]³

³This article was published in Journal of Power Sources, 174, Yang, B. et al., Protective nitride formation on stainless steel alloys for proton exchange membrane fuel cell bipolar plates, 228-236, Copyright Elsevier (2007)

Feng et al. [20] and colleagues investigated the effect of high and low temperature nitrogen plasma immersion ion implantation (PIII) of titanium. No significant effects were discovered for the low temperature PIII compared to the bulk material. Although the high temperature PIII treated specimen showed better results for the corrosion as well as for the interfacial resistance analysis.

Brady et al. [8] and Toops et al. [68] investigated thermal nitridation of stainless steel alloys. They showed that the modified Fe-20Cr-4V possessed the best potential for the usage as bipolar plate materials compared to its untreated material and 904L alloy. In the work done by Hong et al. [32] austenitic steel (316L) was nitrided by inductively coupled plasma using a gas mixture of N₂ and H₂ at relatively low temperatures (~270 °C – 380 °C). The specimen prepared at ~316 °C showed good electrical and electrochemical properties.

5.5 Conductive polymer coating

Extrinsic

An extrinsically conductive material is composed of at least two different components, the binding agent, which is a polymer in general, and the electrical conductive filler. As filler mostly a metallic or carbon powder is used. The amount of the electrical conductive material needs to be high enough so the distance between the particles undermatches 10 nm to bring the composite above the percolation threshold where the conductivity of the composite increases excursively [63].

Carbon nanotubes (CNT) as a layer between steel plate and coating

Yang-Bok Lee and his colleagues [45] showed, that a CNT layer between a stainless steel plate and a coating of a pressure molded polypropylene-graphite-carbon fiber composite decreases the interfacial contact resistance. The best results were reached by direct deposition of the CNT on the plates with a decrease of 90%. The corrosion resistance test results showed that the chosen polymer-composite is a good protection for the stainless steel.

PTFE⁴-Composites with CNT and Ag as electro-conductive filler

Show and Takahashi [66] reported on a CNT/PTFE composite which was coated on a stainless steel bipolar plate in dispersed form. With an amount of 75% of CNT a conductivity of 12 S/cm has been measured. Besides a better corrosion resistance and a decrease in contact resistance between the surface of the modified bipolar plate and the carbon paper 46 mOhm*cm² for bare plates to 12 mOhm*cm² for the coated samples was achieved. A PEMFC equipped with these coated plates reached a 1.6 times higher power output in comparison to a system with uncoated separators.

Another PTFE-composite used as coating material is shown by Yu Fu et al. [22]. In this case an Ag-PTFE composite was electro-deposited on the plate surface. The coated plates showed a similar performance to those of the uncoated ones for the interfacial contact resistance and

⁴ Polytetrafluoroethylen one of the known trademarks is Teflon®

the corrosion stability. An improvement was reported for the contact angle being an important factor in the water management of a fuel cell.

Resin-Composites

A resin-composite-coating was tested by Kitta et al.[38]. They coated a stainless steel plate with a thin composite film of bisphenol A-type epoxy resin and 60 vol.% of graphite. Additionally to the coating they brought a rib structure on the plate using a different resin graphite system. In this case the researchers used a cresol-novolak-type epoxy resin with 70 vol.% of graphite as electrical conductor. The phenol-type hardener showed a high stability at 90 °C. Only a small amount of ionic impurities ($<20 \mu\text{S}/\text{cm}$) was found. The area specific resistance of the described plate was reported as $13.8 \text{ m}\Omega\cdot\text{cm}$ at a tightening force of 1 MPa. Epoxy resins are also found in other applications such as shielding electromagnetic/radio frequency interferences and in dissipating static charges. Azim et al. [4] reported about a composite of polysulfide modified epoxy resin cured with a polyethylene polyamine and carbon based electro-conducting fillers. They showed that at an amount of 55 vol.% of conductive filler in the composite, consisting of 85 % graphite and 15% carbon black, the material had a specific volume resistance $2\cdot 10^{-5} \text{ Ohm}\cdot\text{m}$.

Rubber-Titanium nitride-Composite

Another approach to reduce the interfacial contact resistance of stainless steel bipolar plates is shown by Kumagai, M. et al. [40]. The stainless steel plates were coated with a suspension of TiN and styrene butadiene rubber (SBR) by using electro-phoretal deposition. Fig. 8 compares the degradation by the help of cell voltages over 300 hours in a single cell of treated plates. The diagram shows that the plates coated with TiN/SBR provided voltage losses which were comparable to graphite. As shown in Fig. 7, the TiN/SBR coating enlarges the contact area of the bipolar plate and the gas diffusion layer. This effect is due to the elasticity of the SBR.

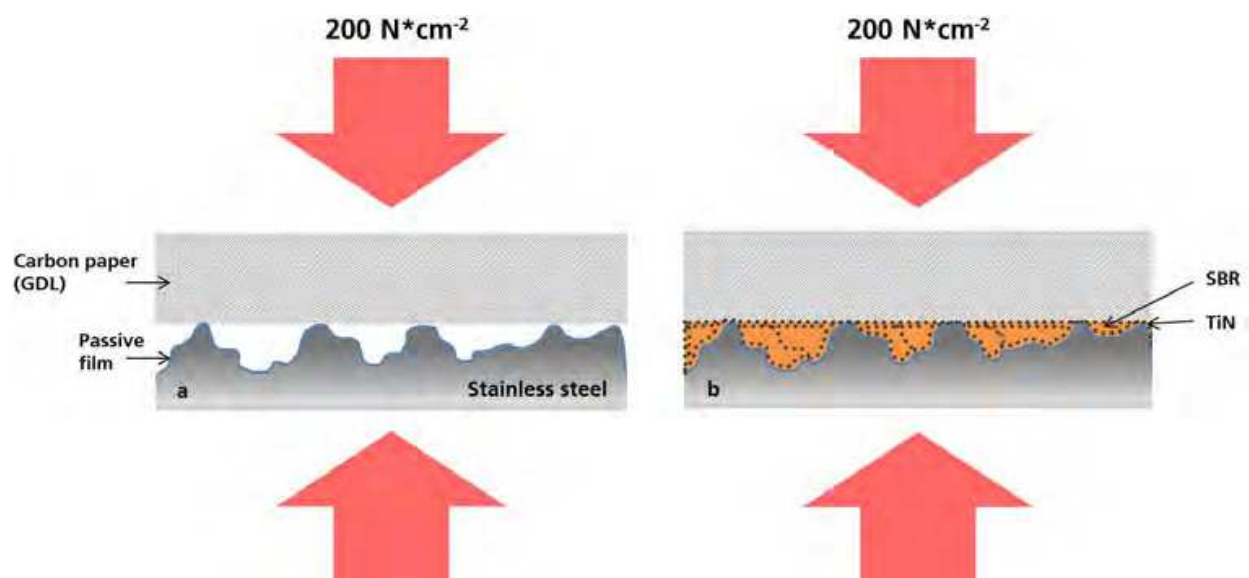


Fig. 9. Effect of TiN/SBR coating (b) on the contact between BPP and GDL in comparison to an as-polished stainless steel (a) [40]

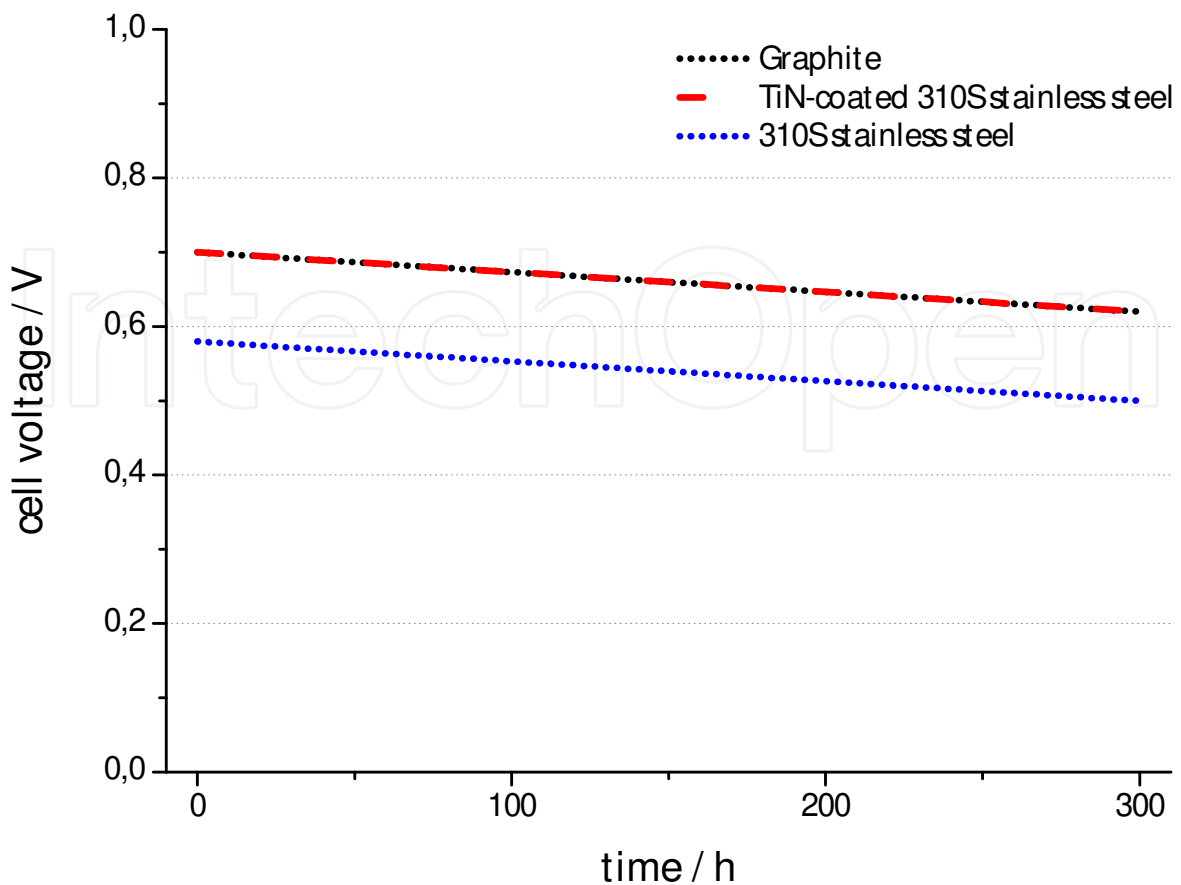


Fig. 10. Qualitative diagram of the cell voltage loss of the treated specimen [40]

Intrinsic

Intrinsically conductive polymers were first discovered by Letheby in 1862. In 2000 the Nobel Prize in Chemistry was given to three scientists who have revolutionized the development of electrically conductive polymers. The conductivity is realized through conjugated double bonds along the backbone of the polymer (seen in Fig. 9, Fig. 10) unlike fillers in extrinsically conductive materials [51]. A very low electrical resistance of these polymers can be reached by oxidation. This procedure is known as “doping” and the effects defect electrons on the conjugated polymer chains.

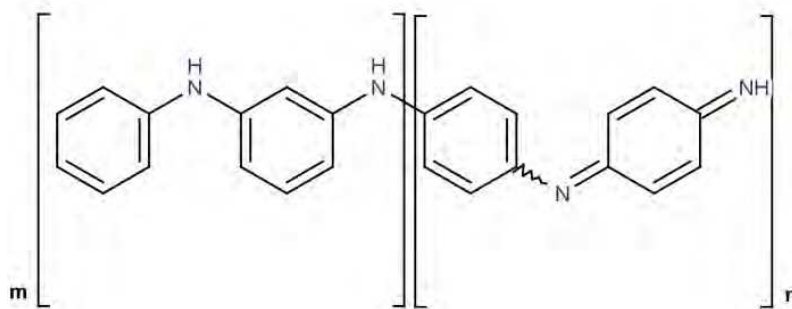


Fig. 11. Chemical structure of Polyaniline (PAni) [7]



Fig. 12. Chemical structure of Poly(pyrrole) PPy (left), Polythiophene (PTh) (right) [7]

Besides the electrical conductivity and light emission of the polymer the corrosion protection properties were also investigated. Different polymers are qualified to be used as corrosion improvements for steels [46]:

- Poly(pyrrole) PPy
- Polythiophene (PTh)
- Polyaniline (PAni)

Ren et al. [59] reported about the coating of stainless steel plates with polypyrrole and polyaniline. The coatings were brought onto the steel surface by galvanostatic deposition for polypyrrole and by cyclic voltametric deposition for polyaniline. The PPy were placed first as an inner layer, following covered by the PAni. Electrochemical measurements showed a better corrosion resistance in 0.3 M HCl for the composite coating compared to a single PPy layer. The coatings increased the potential for corrosion (~ 400 mV) and for pitting corrosion (600 mV) as compared to the bare stainless steel sample. Though the corrosion current was similar to that of the bulk specimen it was rather an indication of the oxidation reduction reaction than the corrosion of the substrate material. The chemical stability for the composite coating was higher than that of the single layer PPy after 36 days exposure to the electrolyte. The contact resistances measurement results for PPy/PAni coating on steel as substrate compared to graphite and uncoated steel is shown in Fig. 11.

Joseph et al. [36] published results comparing PPy and PAni coated stainless steel plates. The coated plates showed improved corrosion resistances in fuel cell environment. Best results for corrosion resistance (~ 350 mV vs. SCE) were achieved after the third deposition cycle. However with increasing of the thickness of the coating the corrosion potential decreased to ~ 120 mV vs. SCE. The contact resistance was higher for the PPy and PAni coated steel samples compared to the bulk substrate.

PPy coatings were electro-polymerized by García et al. [25] and the corrosion properties under fuel cell conditions were investigated. The results show that the coatings are capable of reducing the corrosion current. For room temperature tests the results show a decrease of up to two orders of magnitude and for 60 °C operation temperature of even up to four orders of magnitude. Nevertheless the protective properties did not last for longer times of immersion in an electrolyte of 0.1 M H₂SO₄. Subsequent tests showed the incorporation of polymer particles of DBSA doped PPy into the metal oxide film on the substrate surface.

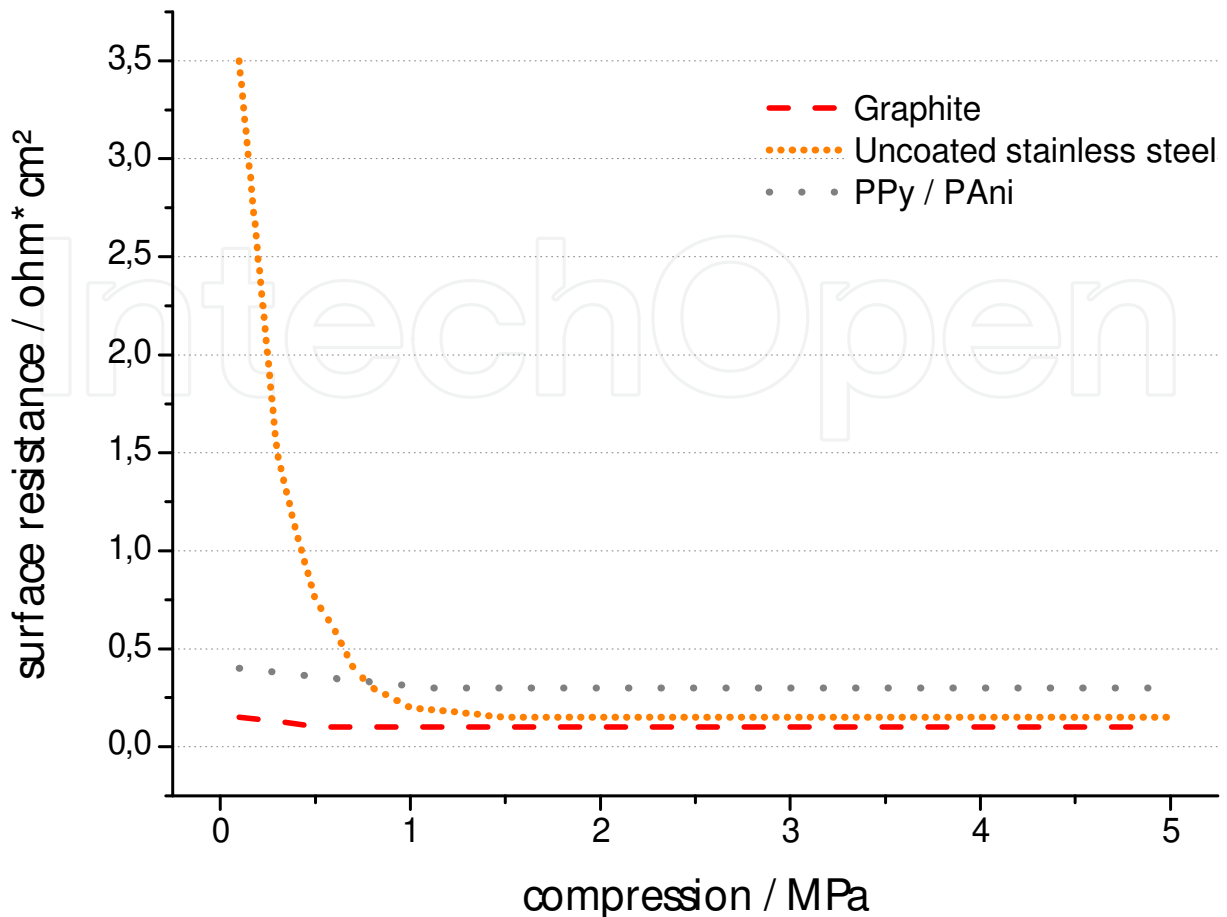


Fig. 13. Contact resistance of the PPy/PANi on stainless steel compared to graphite and uncoated steel [59]

6. Defect detection for coatings

Defects of coatings on metallic bipolar plates can be detected in many different ways. Invasive analytical methods are e.g. the Solid Particle Impact Method, the Colloidal Probe Technique or the Vibration Method [52], [53], [62], [78]. More elegant results are provided by the non-invasive methods such as localized electrochemical impedance spectroscopy (LEIS), the ultrasonic pulse-echo scheme or the scanning kelvin probe. Defects like pinholes as well as high porous coatings are examples for high corrosion currents so they might be detectable directly through an electrochemical corrosion test.

Woo and Wei reported in 1999 [85] a high-fidelity ultrasonic pulse-echo scheme for detecting delamination in thin films. They stated that the influence of surrounding noises can interfere with the results of the analytical method. Another noninvasive method is shown in the work done by Fürbeth et al. [24] and Wielant et al. [82] – the scanning kelvin probe. This technique has been established to detect electrode potentials at buried polymer/oxide/substrate interfaces. The results by Wielant showed a possible correlation between the polymer/iron-oxide peel-off force and the polar surface energy component [82].

Localized EIS, another approach of detecting defects in coatings, is displayed in the work by Dong et al. [16]. The results indicated that the corrosion of coated steel is significantly

influenced by cathodic protection potential and the defect geometry. The work also shows a purely capacitive behavior with a phase angle of 90° for a faultless coated steel electrode over most of the measurement frequencies [15]. An LEIS diagram around a defect in a coating after one day of immersion in an alkaline test solution consisting of 0.05 M Na_2CO_3 , 0.1 NaHCO_3 and 0.1 M NaCl und cathodic potential of -850 mV vs. SCE is shown in Fig. 12.

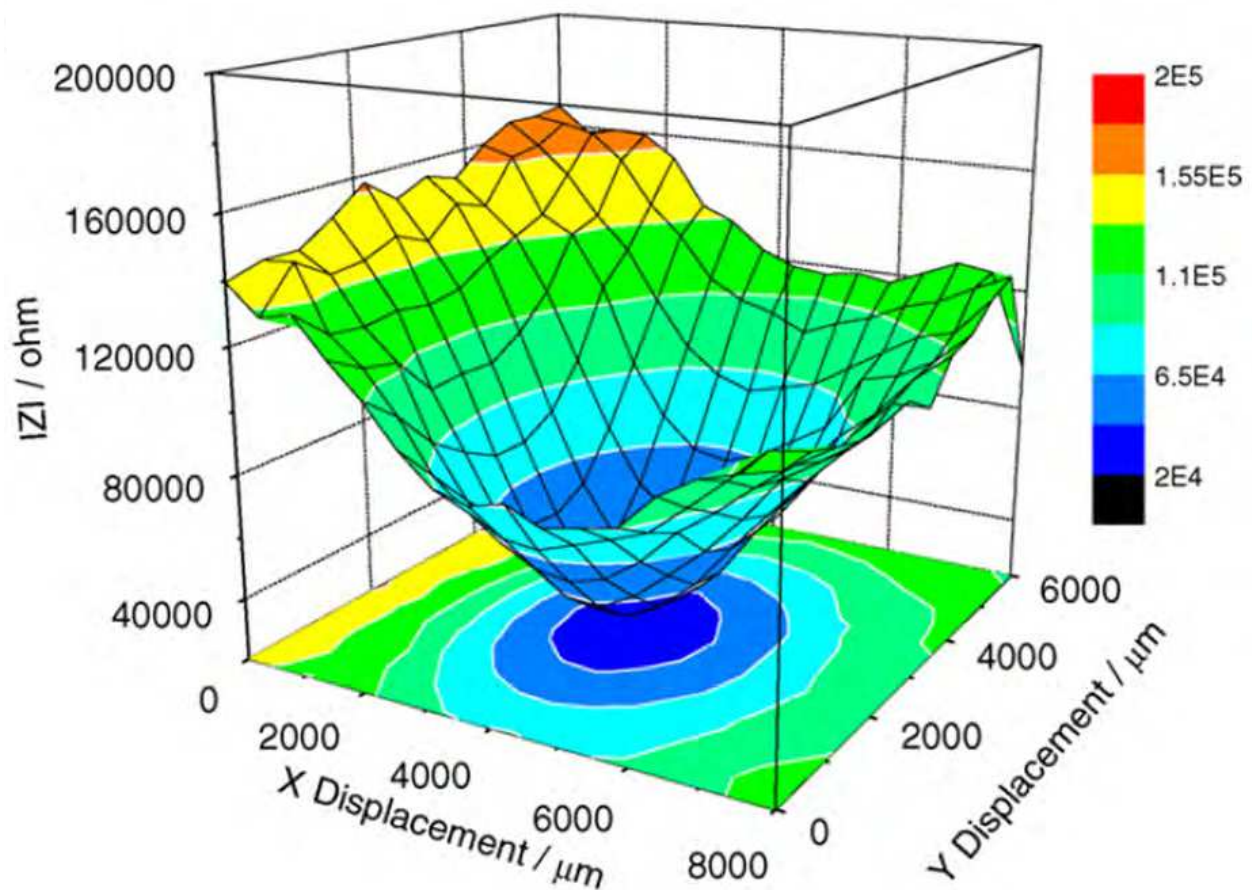


Fig. 14. LEIS maps around the defect [15]⁵

7. Summary and conclusion

Metals as bipolar plates in energy conversion systems offer great opportunities. The high corrosion and the interfacial contact resistance hinder their commercialized usage as substrate materials. During the last decades different approaches were reported by researchers worldwide. To this day it is not clear which the optimal treatment for metals is

⁵This article was published in *Electrochimica Acta*, 54, Dong, C.F. et al., Localized EIS characterization of corrosion of steel at coating defect under cathodic protection, 628-633, Copyright Elsevier (2008)

to resist the harsh environments in an energy conversion system. Many modifications on metals provide good potentials.

Solutions like electro-plating metals or coating them with conductive polymer exhibit similar difficulties by delamination of the coatings. Those defects are mostly noticed through high corrosion currents and degradation of the cells. Modifications on the metal surface through CVD or PVD sometimes show similar challenges for delamination as polymer coatings but they also provide very high corrosion potentials and low contact resistances. Some researcher groups report that the best results are achieved by combining methods like electro-plating and nitration by Wang [74].

For further improvements in surface treatments and for designing new of coatings for metals, noninvasive defect detection methods are a essential research topic. These methods will be able to provide in-situ results for metallic bipolar plates in e.g. fuel cells.

Amorphous metals are possibly the most interesting approach. These bulk metallic glasses provide a good prospect for the use as bipolar plates in energy conversion systems due to their corrosion resistance and manufacturing method. But no long term studies have been made so far.

In former times treating metal alloys to overcome environmental challenges was little more than a niche market. This evolved into a field of greater importance, so that many researchers develop, advance and combine ways to coat metals or even design new metal alloys that exhibit the necessary properties.

8. References

- [1] André, J. et al. *International Journal of Hydrogen Energy* 34 (2009) 3125-3133
- [2] André, J. et al., *International Journal of Hydrogen Energy* 35 (2010) 3684-3697
- [3] Antunes, R. A. et al. *International Journal of Hydrogen Energy* 35 (2010) 3632-3647
- [4] Azim, S. et al., *Progress in Organic Coatings* 55 (2006) 1-4
- [5] Bai, C.-Y. et al., *International Journal of Hydrogen Energy* 34 (2009)
- [6] Berns, H; Theisen, W.; *Eisenwerkstoffe – Stahl und Gusseisen*, 4. Bearbeitete Auflage (2008)
- [7] Bhadra, S. et al. *Progress in Polymer Science* 34 (2009) 783–810
- [8] Brady, M. P. et al. *Journal of Power Sources* 195 (2010) 5610-5618
- [9] California Fuel Cell Partnership, DOE Targets, Webpage:
- [10] <http://www.fuelcellpartnership.org/progress/technology/doetargets>
- [11] Cha, B.-C. et al. *International Journal of hydrogen Energy* 36 (2011) 4565-4572
- [12] Chung, C.-Y., *Journal of Power Sources* 186 (2009) 393–398
- [13] Datz, A. et al., DE 10 2006 017 604 A1 (2007).
- [14] Davies, D.P et al., *Journal of Applied Electrochemistry* 30 (2000) 101-105
- [15] Dong, C.F. et al. *Electrochimica Acta* 54 (2008) 628-633
- [16] Dong, C.F. et al. *Progress in Organic Coatings* 67 (2010) 269-273
- [17] Dur, E. et al. *International Journal of hydrogen Energy* 36 (2011) 7162 – 7173
- [18] El-Enin, S.-A. A. et al. *Journal of Power Sources* 177 (2008) 131-136
- [19] Feng, K. et al. *International Journal of hydrogen Energy* 35 (2010) 690 – 700

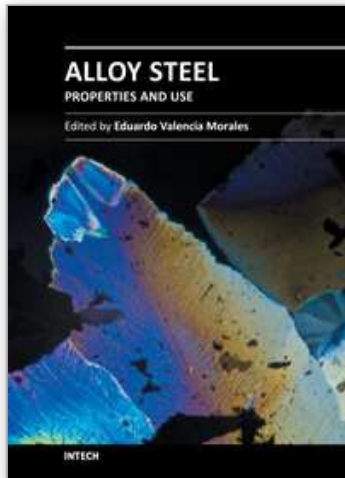
- [20] Feng, K. et al., *Journal of Power Sources* 195 (2010) 6798-6804
- [21] Fu, Y. et al. *International Journal of hydrogen energy* 34 (2009) 405-409
- [22] Fu, Y. et al., *Journal of Power Sources* 182 (2008) 580-584
- [23] *Fuel Cell Handbook - Seventh Edition* (2004)
- [24] Fürbeth, W. et al. *Corrosion Science* 43 (2001) 229-241
- [25] García, L. et al. *Journal of Power Sources* 158 (2006) 397-402
- [26] Georges Leclanché, French Patents, No. 69,980 and 71,865, 1866
- [27] Grove, W. R.; *The London and Edinburgh Philosophical Magazine and Journal of Science - Series 3*, 14 (1839) 127-130
- [28] Henkel, G., *Hinweise zum Passivschichtphänomen bei austenitischen Edelstahllegierungen* (2003)
- [29] Hental, P. L. et al., *Journal of Power Sources* 80 (1999) 235-241
- [30] Heras, N. et al., *Energy & Environmental Science* 2 (2009) 206-214
- [31] Hermann, A. et al., *International Journal of Energy* 30 (2005) 1297-1302
- [32] Hong, W. et al. *International Journal of hydrogen Energy* 36 (2011) 2207-2212
- [33] Jayaraj, J et al. *Material Science and Engineering A* 449-451 (2007) 30-33
- [34] Jayaraj, J et al., *Science and Technology of Advanced Materials* 6 (2005) 282-289
- [35] Jin, S. et al., *Journal of Power Sources* 162 (2006) 294-301
- [36] Joseph, S. et al. *International Journal of Hydrogen Energy* 30 (2005) 1339-1344
- [37] *Journal of Power Sources* 163 (2007) 755-767
- [38] Kitta, S. et al., *Electrochimica Acta* 53 (2007) 2025-2033
- [39] Kravtsov, A. et al. *Journal of Power Sources* 164 (2007) 697-703
- [40] Kumagai, M. et al., *Electrochimica Acta* 54 (2008) 574-581
- [41] Kumagai, M. et al., *Journal of Power Sources* 185 (2008) 815-821
- [42] Lee, S.B. et al. *Journal of Power Sources* 187 (2009) 318-323
- [43] Lee, S.-J. et al. *Journal of Material Processing Technology* 140 (2003) 688-693
- [44] Lee, S.-J. et al., *Journal of Power Sources* 131 (2004) 162-168
- [45] Lee, Y. et al., *International Journal of Hydrogen Energy* 34 (2009) 9781-9787
- [46] Léon C.P. de et al. *Transaction of the Institute of Metal Finishing* 86 (2008) 34-40
- [47] Lin, J.-Y. et al., *Surface Coatings Technology* 205 (2010) 2251-2255
- [48] Linden, D.; Reddy, T.; *Handbook of Batteries - Third Edition* (2002) 1.6
- [49] Mattox, D. M., *Handbook of Physical Vapor Deposition (PVD) Processing - second edition* (2010)
- [50] Miller, M; Liaw, P.; *Bulk metallic glasses - An overview* (2008)
- [51] *Nobel Prize in Chemistry - Conductive Polymers* (2000)
- [52] Oka, Y. et al. *Second International Conference on Erosive and Abrasive Wear*. 258 (2005) 92-99.
- [53] Pashley, D. H. *Dental Materials* 11 (1995) 117-125.
- [54] Pierson, H. O; *Handbook of chemical vapor deposition (CVD) - Principles, Technology, and Application - second edition* (1999)
- [55] Planté, R.G., *Comptes rendus hebdomadaires des séances de l'Académie des sciences* 49 (1859) 402-405
- [56] Poligrat GMBH, Webpage:
- [57] <http://www.poligrat.de/de/Aktuelles/index.htm> (2011)

- [58] Preißlinger-Schweiger, S. et al. EP 1 923 490 A2 (2007).
- [59] Ren, Y.J. et al. Journal of Power Sources 182 (2008) 524-530
- [60] Reuter, M.. Nichtrostende Stähle: Arten, Eigenschaften, Wärmebehandlung, Schädigung. Teil 12 (2001).
- [61] Richards, J. et al. ECS Transactions 25 (2009) 747-755
- [62] Ripperger, S. et al. China Particuology 3 (2005) 3-9
- [63] Rüdiger, D et al. Carbon Leitlacke 148 (2004)
- [64] Schoenbein, C. F., The London and Edinburgh Philosophical Magazine and Journal of Science - Series. 3, 14 (1839) 43-45
- [65] Shao, Y. et al. Journal of Power Sources 167 (2005) 235-242
- [66] Show, Y et al., Journal of Power Sources 190 (2009) 322-325
- [67] Suryanarayana, C.; Inoue, A.; Bulk Metallic Glasses (2011)
- [68] Toops, J. T. et al. Journal of Power Sources 195 (2010) 5619-5627
- [69] Trappmann, C.; Metallische Bipolarplatten für Direkt-Methanol Brennstoffzellen (2010)
- [70] Volta, A; Philosophical Transactions of the Royal Society of London, Vol. 90, pp 403-431, 1800
- [71] Walsh, F.C. et al. Surface & Coatings Technology 202 (2008) 5092-5102
- [72] Wang, Fuel Cell Project Kickoff Meeting – Presentation (2009)
- [73] Wang, H. et al. Journal of Power Sources 138 (2004) 79-85
- [74] Wang, H.; Turner, J.; Corrosion Protection of Metallic Bipolar Plates for Fuel Cells (2006)
- [75] Wang, H.; Turner, J.; Reviewing Metallic PEMFC Bipolar Plates, (2010)
- [76] Wang, J. et al. Surface diffusion modification AISI 304SS stainless steel as bipolar plate material for proton exchange membrane fuel cell, International Journal of hydrogen Energy (2011)
- [77] Wang, Y. et al. Journal of Power Sources 191 (2009) 483-488
- [78] Wang, Y. M. et al. Applied Surface Science 255 (2009) 6875-6880.
- [79] Webpage: <http://www.finanzen.net/rohstoffe> (2011)
- [80] Webpage: <http://www.gold-goldbarren.com/goldpreise/goldpreisentwicklung/> (2011)
- [81] Wen, T.M. et al., Corrosion Science 52 (2010) 3599-3608
- [82] Wielant, J. et al. Corrosion Science 51 (2009) 1664-1670
- [83] Wind, J.; Metallic bipolar plates for PEM fuel cells, Journal of Power Sources 105 (2002) 256-260
- [84] Wonseok, Y.; Evaluation of coated metallic bipolar plates for PEMFC; Journal of Power Sources 179 (2008) 265-273
- [85] Wooh et al. Composites. Part B 30 (1999) 433-441
- [86] Worcester Polytechnic Institute, Project Report: Observation of a Polymer Electrolyte Membrane Fuel Cell Degradation Under Dynamic Load Cycling (2009)
- [87] Yang, B. et al., Journal of Power Sources 174 (2007) 228-236
- [88] Yoon, W. et al., Journal of Power Sources 179 (2008) 265-273
- [89] Zhang, J. et al. Journal of Power Sources 160 (2006) 872-891
- [90] Zhang, M. et al. Journal of Power Sources 196 (2011) 3249-3254

- [91] Ziomek-Moroz, M.; Corrosion behavior of stainless steel in solid oxide fuel cell simulated gaseous environments DOE (2003)

IntechOpen

IntechOpen



Alloy Steel - Properties and Use

Edited by Dr. Eduardo Valencia Morales

ISBN 978-953-307-484-9

Hard cover, 270 pages

Publisher InTech

Published online 22, December, 2011

Published in print edition December, 2011

The sections in this book are devoted to new approaches and usages of stainless steels, the influence of the environments on the behavior of certain classes of steels, new structural concepts to understand some fatigue processes, new insight on strengthening mechanisms, and toughness in microalloyed steels. The kinetics during tempering in low-alloy steels is also discussed through a new set-up that uses a modified Avrami formalism.

How to reference

In order to correctly reference this scholarly work, feel free to copy and paste the following:

J. Richards and K. Schmidt (2011). Review – Metallic Bipolar Plates and Their Usage in Energy Conversion Systems, Alloy Steel - Properties and Use, Dr. Eduardo Valencia Morales (Ed.), ISBN: 978-953-307-484-9, InTech, Available from: <http://www.intechopen.com/books/alloy-steel-properties-and-use/review-metallic-bipolar-plates-and-their-usage-in-energy-conversion-systems>

INTECH
open science | open minds

InTech Europe

University Campus STeP Ri
Slavka Krautzeka 83/A
51000 Rijeka, Croatia
Phone: +385 (51) 770 447
Fax: +385 (51) 686 166
www.intechopen.com

InTech China

Unit 405, Office Block, Hotel Equatorial Shanghai
No.65, Yan An Road (West), Shanghai, 200040, China
中国上海市延安西路65号上海国际贵都大饭店办公楼405单元
Phone: +86-21-62489820
Fax: +86-21-62489821

© 2011 The Author(s). Licensee IntechOpen. This is an open access article distributed under the terms of the [Creative Commons Attribution 3.0 License](#), which permits unrestricted use, distribution, and reproduction in any medium, provided the original work is properly cited.

IntechOpen

IntechOpen